

Capillary solution evaporation theory is presented, which incorporates crystal formation near the mouth when supersaturation is reached; high evaporation rates and high solution concentrations can result in a transient state, where the crystal size pulsates.

An aqueous solution evaporating from a capillary for $p_0 < p_m$ produces a gradual increase in the nonvolatile-component concentration (e.g., salt) near the meniscus; the salt diffuses back into the capillary if the meniscus position is unchanged (by solution supply), and a stationary state occurs, with a certain constant value $C_m > C_0$ [1, 2].

At high evaporation rates, C_m may exceed C_s , which leads to crystals being deposited, as observed for aqueous solutions of potassium dichromate in glass capillaries [3]. The crystals narrow the capillary, which reduces the evaporation rate and correspondingly the flow speed. However, a lower v corresponds to a smaller C_m , which may become less than C_s , so the crystal partly dissolves. A crystal volume reduction again increases the evaporation rate, so the concentration rises again near the meniscus, which may cause the crystal to grow. The transition to the stationary state may involve crystal volume oscillations.

The oscillating conditions may be established by considering the evaporation of an aqueous salt solution (Fig. 1); the meniscus is in a fixed position, which is provided, as in [3], by narrowing at the end and the liquid being drawn up to the mouth. The capillary communicates with the vessel maintaining a constant concentration C_0 . The condition $L \gg r_0$ allows one to neglect edge effects.

Convection in the air near the mouth produces a diffusion layer, thickness δ , within which the vapor pressure falls linearly from p_m to p_0 [4]. The evaporation rate is then defined by the diffusion equation

$$\alpha = \frac{D_0 v_m}{RT\delta} (p_m - p_0). \quad (1)$$

The concentration distribution $C(x)$ along the capillary is found by solving the convective-diffusion equation for the salt flux:

$$Q = \pi r_0^2 \left(-D \frac{\partial C}{\partial x} + vC \right). \quad (2)$$

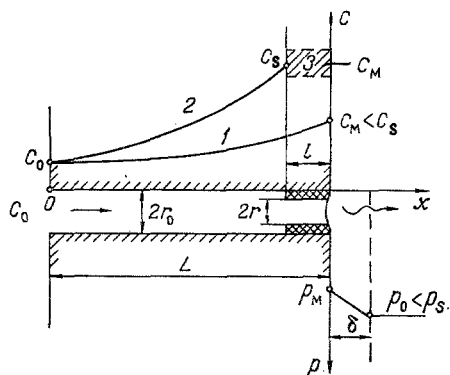


Fig. 1. Working scheme and salt concentration distribution along capillary with subsaturation (1) and supersaturation (2) near the mouth (3 is the crystallization zone).

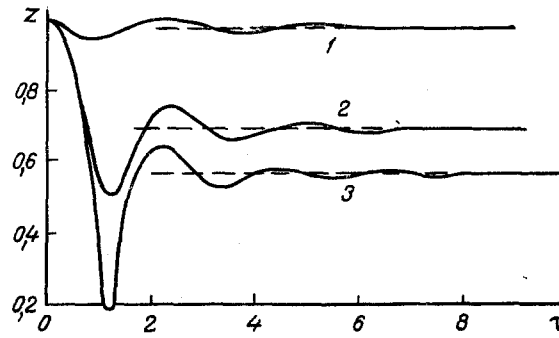


Fig. 2. Capillary narrowing by a growing crystal for $\gamma = 2.4$ (1); 4.8 (2); 7.2 (3).

The boundary conditions are $C(0) = C_0$, $C(L) = C_m$ and $dC/dx(0) = 0$.

If $C_m < C_s$, the salt flux in the stationary state is zero; the solution to (2) here gives for $C_m = \text{constant}$ the standard expression [1, 2]

$$C_m = C_0 \exp(\alpha L/D). \quad (3)$$

Curve 1 in Fig. 1 shows the corresponding $C(x)$; at higher evaporation rates, C_m may attain C_s , which allows a crystal to form and grow; experiment shows that the crystallization is heterogeneous, at the capillary walls [3]. We assume for simplicity that a crystalline phase is formed as shown in Fig. 1 in a certain zone of constant length ℓ . The crystal is assumed to grow in layers, so the channel gradually narrows to $r < r_0$. Then $r_0 - r$ characterizes the layer thickness. The situation ceases to be stationary, since the crystal grows for a time t , so the flux Q , flow speed v , and radius of the free part r are functions of time.

Here we give a solution for the growth beginning when C_m becomes equal to C_s at the end of zone ℓ , i.e., at $x = L - \ell$; that state occurs after about $\Delta t = 2C_s D/3C_0 \alpha^2$, and during the subsequent evaporation, the concentration in ℓ begins to exceed C_s , so a crystal can form and grow.

The growing crystal reduces the evaporation area, so (2) is rewritten as

$$Q = \pi r_0^2 \left[-D \frac{\partial C}{\partial x} + \alpha C \left(\frac{r}{r_0} \right)^2 \right]. \quad (4)$$

Here v is expressed in terms of the evaporation rate as the fluxes are equal: $\pi r_0^2 v = \pi r^2 \alpha$; the evaporation flux is proportional to πr^2 , so any reduction in α reduces the flow speed. For each t , the solution to (4) in the quasistationary approximation for the salt flux to the meniscus is

$$Q_m(t) = (\alpha \pi r^2) \frac{C_s - C_0 \exp(\alpha r^2 L/r_0^2 D)}{1 - \exp(\alpha r^2 L/r_0^2 D)}. \quad (5)$$

Q_m is a function of the current radius $r(t)$; the boundary condition is that the concentration at the entry to the crystallization zone is equal to the saturation concentration $C_s = \text{constant}$ (curve 2, Fig. 1). $Q_m(t)$ is consumed in altering the crystal mass M_c and the dissolved substance mass M_d in zone ℓ . C_m there is taken as constant (matched zone 3 in Fig. 1), so we have

$$Q_m(t) = \frac{d(M_c + M_d)}{dt} = \frac{d}{dt} [\pi (r_0^2 - r^2) \rho \ell + \pi r^2 \ell C_m(t)]. \quad (6)$$

The growth rate in ℓ is determined by the mass transfer coefficient β :

$$\frac{dr}{dt} = -\frac{\beta}{\rho} [C_m(t) - C_s]. \quad (7)$$

If C_m equals C_s , the crystal is in equilibrium and $dr/dt = 0$; for $C_m(t) \neq C_s$, the crystal either grows or dissolves.

System (5)-(7) represents the volume change; we introduce dimensionless variables and parameters for convenience: $z = r/r_0$; $\tau = t/t_0$; where $t_0 = 2\rho \ell / C_0 \alpha$; $y = C_m(t)/C_s$; $\gamma = \alpha L/D$; $\lambda = C_s/C_0 > 1$; $\varepsilon = C_s/\rho$; $\nu = C_s \beta t_0 / \rho r_0$. Then (5)-(7) becomes

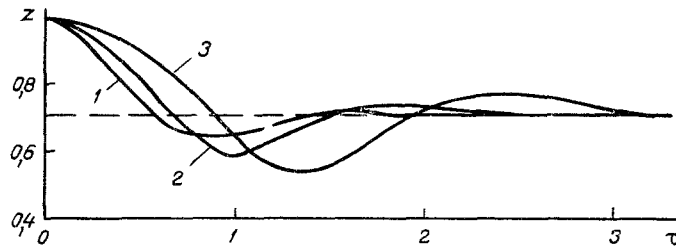


Fig. 3. Effects of v/ε on growth kinetics for $\gamma = 4.6$ and $\lambda = 10$: $v/\varepsilon = 0.5$ (1); 1 (2); 2 (3).

$$-\dot{z}(1-\varepsilon y) + \frac{\varepsilon}{2} z \dot{y} = z \left(\frac{\lambda - \exp \gamma z^2}{1 - \exp \gamma z^2} \right); \quad (8)$$

$$\dot{z} = -v(y-1), \quad (9)$$

where \dot{z} and \dot{y} are the first derivatives with respect to τ . The initial conditions for this system are $z(0) = 1$, $\dot{z}(0) = 0$, and $y(0) = 1$.

We differentiate (9) with respect to τ : $\ddot{z} = -v\dot{y}$ and substitute into (8) to get

$$\ddot{z} + \frac{2v(1-\varepsilon)}{\varepsilon} \frac{\dot{z}}{z} + 2 \frac{\dot{z}^2}{z} + \left(\frac{2v}{\varepsilon} \right) \left[\frac{\exp(\gamma z^2) - \lambda}{\exp(\gamma z^2) - 1} \right] = 0. \quad (10)$$

For $\tau \rightarrow \infty$, we get a stationary state, where $y(\infty) = 1$ and $C_m = C_s = \text{const}$; this is maintained because the convective mass input to the meniscus is equal to the reverse diffusion flux, and then (7) shows the $dr/dt = 0$, which corresponds to an unchanging volume. This may be characterized by $z(\infty) = \sqrt{(1/\gamma) \ln \lambda}$ or $r(\infty)/r_0 = \sqrt{(D/\alpha L) \ln(C_s/C_0)}$.

We now consider how this stationary state may be approached. We solve (10) numerically with the following parameters: $v/\varepsilon = 2\beta\rho\ell/C_0r_0\alpha = 0.5$ and $\lambda = 10$, which corresponds to a solution concentration C_0 less than C_s by an order of magnitude.

Figure 2 shows calculations on the narrowing during evaporation; the abscissa is the dimensionless time τ and the ordinate $z = r/r_0$. Then there is no crystal for $z = 1$ and $\tau = 0$: $r = r_0$. For $\tau \rightarrow \infty$, a constant-thickness layer is formed, which is governed by $\gamma = \alpha L/D$, which takes the values 2.4 (curve 1), 4.8 (curve 2), and 7.2 (curve 3). Increase in the evaporation rate and/or capillary length under otherwise equal conditions raises the oscillation amplitude. For $\gamma = 7.2$, the channel is almost completely blocked ($z = 0.18$). In fact, it is found that the crystal rapidly fills the channel when the evaporation rate increases [3], while when γ is less by only a factor 3 (curve 1), the pulsations are almost inappreciable. With a low evaporation rate, a thin layer is sufficient to give the stationary state.

Figure 3 shows analogous $z(\tau)$ curves illustrating the effects of v/ε ; when this increases, so does the pulsation amplitude, while the settling time lengthens. Here v/ε characterizes largely the evaporation rate α and C_0 , since ℓ should be of the order of r_0 , while ρ and β can be taken as constant, so we conclude that the transient oscillation is the more prolonged the lower the evaporation rate and the lower the initial concentration.

We can now estimate the settling and blocking times; we take the initial $K_2Cr_2O_7$ concentration such that $\lambda = 10$, and as $C_s = 0.13 \text{ g/cm}^3$, we take $C_0 = 1.3 \cdot 10^{-2} \text{ g/cm}^3$. With $\ell \approx r_0 = 10^{-3} \text{ cm}$ and $\rho = 2.7 \text{ g/cm}^3$, we get the characteristic time as $t_0 = 0.4/\alpha$. We derive α from (1) with the values for water: $v_m = 18 \text{ cm}^3/\text{mole}$, $D_0 = 0.25 \text{ cm}^2/\text{sec}$, and $\varepsilon = 0.1 \text{ cm}$ [4]. Laboratory conditions are assumed ($p_0/p_m = 0.5$), with $\alpha = 2 \cdot 10^{-5} \text{ cm/sec}$, which gives t_0 as $2 \cdot 10^4 \text{ sec}$ or about 5.5 h. With $L = 7 \text{ cm}$, $\alpha = 2 \cdot 10^{-5}$ (with $D = 2 \cdot 10^{-5} \text{ cm}^2/\text{sec}$) corresponds to $\gamma = 7$. For this γ (curve 3 in Fig. 2), the channel should be blocked for $t/t_0 = 1.2$, i.e., in about 7 h. Experiment showed blocking in a day [3], but the measurements were made with a weaker solution ($C_0 \leq 5 \cdot 10^{-3} \text{ g/cm}^3$), and Fig. 3 shows that this should increase the blocking time.

Raised temperatures increase primarily the evaporation rate and should shorten the onset of crystallization considerably.

These solutions illustrate ways of controlling crystallization on evaporation from a capillary; to suppress crystallization, one has to reduce the evaporation rate or capillary

length and thus facilitate the diffusion of the nonvolatile component accumulating at the meniscus. The danger of crystals depositing will be the smaller the lower the initial concentration. One can use (10) to estimate the effects of all these factors.

Crystals can form when C_m rises to C_s ; (3) shows that the crystallization condition can be put approximately as $\alpha \leq (D/L) \ln C_s/C_0$, which defines an evaporation rate above which crystals may be formed.

NOTATION

C_0 , initial concentration; C_m , concentration near meniscus; p_0 and p_m , vapor partial pressures in the surroundings and above the meniscus; C_s , saturation concentration; L , capillary length; r_0 , capillary radius; v , flow speed in capillary; α , volume evaporation rate from unit surface, cm/sec; v_m , molar volume of water; R , gas constant; T , temperature, K; Q , salt flux, g/sec; D , salt diffusion coefficient in solution; D_0 , vapor diffusion coefficient in air; t , time; ρ , crystal density.

LITERATURE CITED

1. P. P. Zolotarev, Dokl. Akad. Nauk SSSR, 168, No. 1, 83-87 (1966).
2. R. A. Tishkova, N. V. Churaev, and A. P. Ershov, Inzh.-Fiz. Zh., 37, No. 5, 849-853 (1979).
3. K. B. Yatsimirskii, L. I. Budarin, A. F. Verlan', et al., Dokl. AN Ukr. SSR, Ser. Geol., Khim. Biol. Nauk, No. 8, 56-59 (1982).
4. A. V. Lykov, Heat and Mass Transfer in Drying [in Russian], Moscow-Leningrad (1956), p. 137.

EFFECTS OF GROWTH RATE PULSATIONS IN BULK-CRYSTALLIZATION OSCILLATIONS

Yu. A. Buevich and I. A. Natalukha

UDC 541.48:66.065.5-51

Weakly nonlinear periodic bulk crystallization conditions are examined in the presence of growth rate fluctuations.

It has been shown [1] that bulk crystallization in a supersaturated or supercooled liquid can give rise to oscillations if the nucleation frequency has a markedly nonlinear relation to the metastability, where the transition to the oscillatory state occurs as a result of normal Hopf bifurcation in the stationary states. It was assumed [1] that each crystal arising in the bulk grows monotonically without rate fluctuations, which is characteristic of many actual processes. However, recent measurements show that growth rates can fluctuate under certain conditions, which may be due to instability in external conditions, e.g., microscopic inhomogeneity or substances active in adsorption [2], or to various processes at the faces such as microrelief change [3] or alternation in defectiveness associated with Frank-Read sources periodically generating dislocation loops [4, 5]. When the growth-rate fluctuations are major, the crystallization acquires some novel features not explicable from the classical model [6, 7]. For example, instead of a monodisperse composition expected for heterogeneous crystallization on ready-made microcrystals of the same size (where nuclei do not arise by fluctuation), and where the nuclei are involved in growth immediately on introduction and grow without forming additional particles, one often gets a resultant distribution with marked size variation [8], which indicates a spread in growth rates. Under certain conditions, the size curves tend to spread as time passes [2, 3, 9-11]. This is also not explicable from the classical theory. The model has been altered to incorporate rate pulsations around the mean, which has explained [2, 3, 9] the distribution spread and the considerable positive skewness, as well as the deformation towards large sizes.

Gorkii Urals University, Sverdlovsk. Translated from Inzhenerno-Fizicheskii Zhurnal, Vol. 54, No. 4, pp. 640-648, April, 1988. Original article submitted December 1, 1986.